Nanocomposites and polyethylene blends: two potentially synergistic strategies for HVDC insulation materials with ultra-low electrical conductivity

N.B. When citing this work, cite the original published paper.

(article starts on next page)

Nanocomposites and polyethylene blends: two potentially synergistic strategies for HVDC insulation materials with ultra-low electrical conductivity

Fritjof Nilsson [a,*], Mattias Karlsson [a], Ulf W. Gedde [a], Roland Kádár [b], Karolina Gaska [c], Christian Müller [e], Per-Ola Hagstrand [d], Richard T. Olsson [a], Mikael S. Hedenqvist [a], Thomas Gkourmpis [d]

[a] *Department of Fibre and Polymer Technology, School of Engineering Sciences in Chemistry, Biotechnology and Health, KTH Royal Institute of Technology, SE-10044, Stockholm, Sweden*
[b] *Department of Industrial and Materials Science, Engineering Materials. Chalmers University of Technology, SE-41296, Gothenburg, Sweden*
[c] *Department of Aerospace Engineering, University of Bristol, Bristol BS8 1TR, UK*
[d] *Innovation &Technology, Borealis AB, SE-44486, Stenungsund, Sweden*
[e] *Department of Chemistry and Chemical Engineering, Chalmers University of Technology, SE-41296, Gothenburg, Sweden*

ARTICLE INFO

ABSTRACT

Among the various requirements that high voltage direct current (HVDC) insulation materials need to satisfy, sufficiently low electrical conductivity is one of the most important. The leading commercial HVDC insulation material is currently an exceptionally clean cross-linked low-density polyethylene (XLPE). Previous studies have reported that the DC-conductivity of low-density polyethylene (LDPE) can be markedly reduced either by including a fraction of high-density polyethylene (HDPE) or by adding a small amount of a well dispersed, semiconducting nanofiller such as Al_2O_3 coated with a silane. This study demonstrates that by combining these two strategies a synergistic effect can be achieved, resulting in an insulation material with an ultra-low electrical conductivity. The addition of both HDPE and C_8–Al_2O_3 nanoparticles to LDPE resulted in ultra-insulating nanocomposites with a conductivity around 500 times lower than of the neat LDPE at an electric field of 32 kV/mm and 60–90 °C. The new nanocomposite is thus a promising material regarding the electrical conductivity and it can be further optimized since the polyethylene blend and the nanoparticles can be improved independently.

1. Introduction

The growing global demand for renewable sources of energy increases the need for transporting electrical energy over large distances with minimal losses [1]. High-voltage direct current (HVDC) transmission lines are most efficient [2–4]. Air-insulated electrical overhead cables can be used in areas with few inhabitants, but in highly populated areas and when traversing oceans, the cables must be surrounded by an insulating layer. A high voltage is desired since a doubling of the voltage reduces the electrical losses by a factor of four. However, thermal and electrical stresses on the insulating material also increase rapidly with increasing voltage, which necessitates insulating materials with excellent physical properties. A suitable HVDC insulation material should

have good thermal and mechanical properties as well as excellent electrical characteristics – high electrical breakdown strength, low dielectric permittivity, low space charge accumulation, low tendency for electrical treeing, low electric conductivity – in order to fulfil the demanding long-term requirements [2,5]. Among these requirements, an exceedingly low electrical conductivity is particularly important [6–8].

Traditionally, modern commercial extruded HVDC cables are made of extruded low-density polyethylene (LDPE), which is cross-linked into XLPE to increase its thermomechanical stability [9]. Recent studies have revealed that the DC-conductivity of LDPE can be reduced using either of two strategies: Firstly, if a small fraction (2–10 wt%) of high-density polyethylene (HDPE) is added to the LDPE, the resulting LDPE/HDPE

---

blend has a conductivity nearly one order of magnitude lower than that of the pure LDPE [10], with a reduced space charge accumulation [11] and an greater thermal stability [12]. Secondly, if a small amount (1–5 wt%) of inorganic nanoparticles such as Al_2O_3 [13], MgO [6], ZnO [7,8] or SiO_2 [14–16] are dispersed in LDPE, the electrical conductivity can be reduced by approximately two orders of magnitude. The addition of Al_2O_3 nanoparticles to a polyolefin matrix can also improve other material properties, including a reduction of the thermal resistivity [17,18], the space charge accumulation [19–22] and the dielectric permittivity [23,24]. Further, an increase in the dielectric breakdown strength [19–21,25], the elastic modulus [26,27], the tensile strength [28] and the thermal stability [27] has been reported.

The underlying mechanisms behind the two strategies for reducing the conductivity are still not clear, but several hypotheses have been proposed. Well dispersed nanoparticles in a LDPE matrix can attract small, charge carrying molecules (e.g. ions, polar molecules etc.) and thus have a cleaning action on the polymer, leading to an overall reduction of the electrical conductivity [29,30]. On the other hand, the conductivity of the nanocomposite is also more sensitive to humidity than neat LDPE [29,31–35]. In addition, free electrons and holes can become trapped in deep traps close to the nanoparticle surfaces [17,36, 37], and charge carriers can recombine at the surfaces [38], resulting in fewer space charges. Several reviews on nanodielectrics are available [8, 14,39–44].

The addition of a small fraction of HDPE into the LDPE matrix changes the crystalline structure of the polymer, resulting in phase-separated crystals, an increase in the average thickness of the crystal lamellae [10] and improved thermomechanical properties [12,18]. The thickening of the crystals influences the amount of crystal bridging tie-chains and trapped entanglements [45,46], and this affects the charge distribution in the polyethylene [47]. The HDPE crystals may thus act as deep electron traps [10]. A further reduction in conductivity can be anticipated if the HDPE crystals grow very wide in the LDPE, introducing a labyrinth effect that can impede the charge carriers. Moreover, a reduction in electrical conductivity can occur if the HDPE limits the development of spherulitic structures [48–51]. If both the microstructure and the crystal nanostructure are optimized, the electrical properties can be significantly improved for polyethylene [48] and also for other polyolefin copolymers and blends [52,53]. One further advantage of the use of HDPE is that it allows for an increase in the thermomechanical properties, thus leading to a system that exhibits partial physical crosslinking behaviour without the need of a peroxide [12,18].

The aim of the present study has been to combine these two successful strategies in order to see whether a further reduction in conductivity can be achieved by adding both HDPE and octyl-coated Al_2O_3 nanoparticles to LDPE. If an additive or synergetic effect were observed, this would indicate that the conductivity reductions with HDPE and nanoparticles are due to two different mechanisms and thus that the polymer matrix and the nanoparticles have the potential to be optimized independently.

2. Experimental

Composites of C_8–Al_2O_3, HDPE and LDPE were manufactured and then analysed with transmission electron microscopy (TEM), infrared spectroscopy (IR), scanning electron microscopy (SEM), differential scanning calorimetry (DSC), dynamic mechanical thermal analysis (DMTA) and direct current (DC) electrical conductivity measurements. The materials studied contained 3 wt% nanoparticles because this filler concentration yields, according to earlier studies [29], a material with the lowest electrical conductivity. In order to minimize the number of unknowns in the experiments, the composites were not cross-linked, in contrast to commercial HVDC polyethylene insulation.

3. Material preparation

LDPE (M_w = 117 kg/mol, M_W/M_n = 9, branching fraction 1.9 per 1000 carbons) and HDPE (M_w = 58 kg/mol, M_w/M_n = 6) supplied by Borealis, were used as the matrix materials of the nanocomposites. Aluminium oxide nanoparticles (Nanodur from Nanophase Inc, CAS number 1344-28-01, density 3.97 g/cm³) coated with octyltriethoxysilane (Sigma-Aldrich, CAS-number 3069-42-9) [13] (C_8–Al_2O_3) were used as the filler material. The C_8 coating was obtained by dispersing the Al_2O_3 nanoparticles (3.84 g) in water (163.2 mL) and 2-propanol (753.6 mL) followed by the addition of a 25% ammonia solution (20.4 mL) and silane (21.6 mL). The reaction was carried out for 24 h at room temperature and the coated particles were washed thrice by centrifugation (Rotina 420) at 4500 rpm for 8 min and dispersed in ethanol. The cleaned particles were finally dried overnight at 80 °C and ground with a pestle and mortar into a fine powder [54]. The average diameter of the spherical Al_2O_3 nanoparticles was 50 nm according to TEM [55]. Prior to nanocomposite preparation, the nanoparticles were dried for 20 h at 80 °C in a vacuum oven (Vacucell, MMM group). The dried modified nanoparticles were dispersed in n-heptane (0.3 mL n-heptane per 1 g polymer) and ultrasonicated for 5 min, after which 0.02 wt% antioxidant (Irganox 1076, Ciba Speciality Chemicals, CAS number 2082-79-3) was added. After the LDPE/HDPE powder had been added to the suspension, the slurry was shaken for 1 h with a Vortex Genie 2 shaker (Scientific Instruments Inc) and dried overnight at 80 °C. After being dried, the powder was shaken for another 30 min and then extruded for 6 min at 150 °C and 100 rpm (Micro 5 cc twin screw compounder, Xplore instruments). This material was dried overnight at 80 °C in a vacuum oven. The extruded material intended for DC-conductivity measurements was cut into 2–3 mm pellets and compression moulded (TP400 laboratory press, Fontijne Grotnes BV) to circular films 0.3 mm thick and with a diameter of 75 mm diameter, using a force of 200 kN at 150 °C for 10 min followed by cooling (20 °C/min) to room temperature. The samples were stored in a desiccator between manufacture and measurement.

3.1. Material characterization

Transmission electron microscopy (TEM) (Hitachi HT7700 TEM) was used to confirm that an octyl-silane-coating was present on the spherical nanoparticles. Infrared spectroscopy (IR) (PerkinElmer FTIR spectrum 100) was used as a complement in order to verify the molecular structure of the coated particles.

Scanning electron microscopy (SEM) (Hitachi S-4800 field emission scanning electron microscope) was used to access the nanoparticle dispersion in the composite samples and to examine their crystalline structures. The fractured samples used for the analyses were obtained by cooling 0.3 mm thick samples in liquid nitrogen and then breaking them. Prior to the SEM analysis, the samples were etched for 1 h in a solution of 10 mg $KMnO_4$ in 1 mL acid (10:4:1H_2SO_4:H_3PO_4:H_2O), in order to reveal the crystal structures. The etched samples were washed with water and a conductive platinum layer was sputtered onto the samples for 30 s in an argon atmosphere using a high-resolution sputter coater (Cressington 208RH).

Differential scanning calorimetry (DSC) measurements (Mettler-Toledo DSC 1) were used to determine the crystallinity of the materials. The DSC scans were from 160 to – 20 °C, using a cooling rate of 10 °C/min. (First cooled to – 20 °C at high speed, then heated to 160 °C at 10 °C/min, then cooled to – 20 °C using a cooling rate of 10 °C/min and finally heated to 160 °C again with a heating rate of 10 °C/min) The effect of changing the cooling rate from 1 °C/min to 40 °C/min was also examined. The mass crystallinity w_c was calculated from the DSC curves using the total enthalpy method [56]:

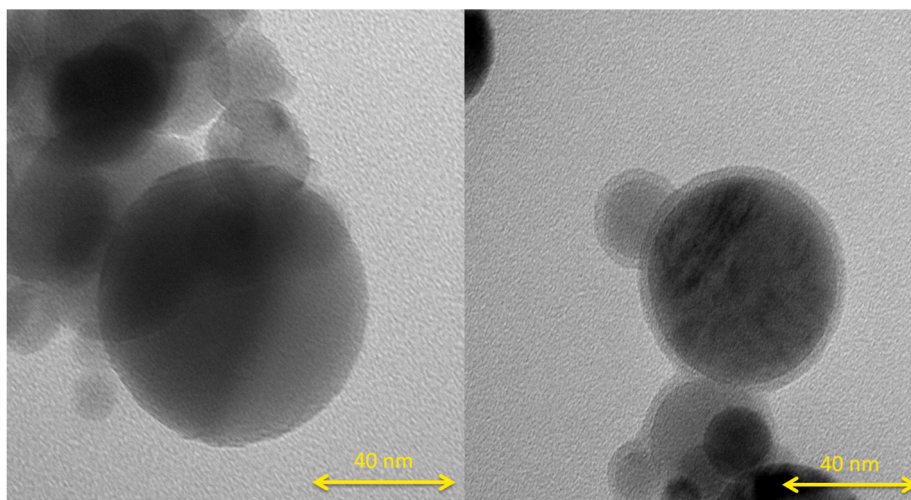$$w_c = \frac{\Delta h}{\Delta h^0(T_1)} \tag{1}$$

Fig. 1. TEM images of unmodified Al_2O_3 (left) and C_8–Al_2O_3 (right) nanoparticles.

where Δh is the measured melting enthalpy, obtained by integrating the melting peak from the onset of melting temperature (T_1) to 160 °C. T_1 is the intersection between the DSC curve and the straight line after the melting peak. The enthalpy of fusion Δh^0 (T_1) was computed as:

$$\Delta h^0(T_1) = \Delta h^0(T_m^0) - \int_{T_1}^{T_m^0} (c_{p,a} - c_{p,c})dT \qquad (2)$$

The equilibrium melting temperature for PE is $T_m^0 = 414.6$ K [57] and the enthalpy of melting for a 100% crystalline PE at T_m^0 is $\Delta h^0(T_m^0) = 286.7$ J/g [58]). The temperature dependent heat capacities for the amorphous and crystalline parts of the PE are denoted $c_{p,a}$ and $c_{p,c}$, respectively. With known heat capacities for PE [57], Δh^0 (T_1) (J/g) can (in the range 250 K–414.6 K) be approximated by:

$$\Delta h^0(T_1) \approx 286.6 - 0.1721 \left(497 + 3.043 \ T_1 - 0.0238 \ T_1^2 + 0.0000328 \ T_1^3\right) \qquad (3)$$

Torsional dynamic mechanical thermal analysis (DMTA) was performed using an Anton Paar MCR702 TwinDrive (Graz, Austria) rheometer operating in the single motor-transducer configuration (stress-controlled). A SCF cylindrical sample fixture was used, with the temperature being controlled via a CTD450 convection oven. The temperature was increased from 30 to 130 °C at a rate of 2 °C/min while the samples were subjected to a 1% strain amplitude at a frequency of 0.8 Hz. The test samples were prepared directly from extruded strands (3 mm in diameter) by cutting to a total length of 40 mm, so that the free sample length was ca. 26 mm.

DC-conductivity measurements were performed at 60, 70 and 90 °C in a measurement cell, placed in a Binder FED 115 oven, where the voltage (32 kV/mm) was generated with a FUG HCP 35–12500 generator and the signals were measured using a Keithley 6517B electrometer. A stainless-steel high-voltage electrode, equipped with brass sensing (30 mm in diameter) and guard electrodes, was used. The signals were sampled and controlled with Labview. Two measurements at each material and temperature were typically used to control the repeatability of the measurements. A randomized order of the measurements was used to reduce the effects of systematic errors. The samples were placed in the measurement chamber 1 h before the measurements to ensure that the desired temperature was reached. The output from the conductivity measurement cell was electrical current I (A). The currents were converted to conductivity (S/m) using the equation $\sigma = LI/(U\pi r^2)$, where σ is the conductivity (in S/m), $r = 0.015$ m is the radius of the sensing electrode, $L = 280 \pm 7$ μm is the thickness of the sample, $U = 9000$ V is the applied voltage and $E = U/L = 32$ kV/mm is the electric field. The

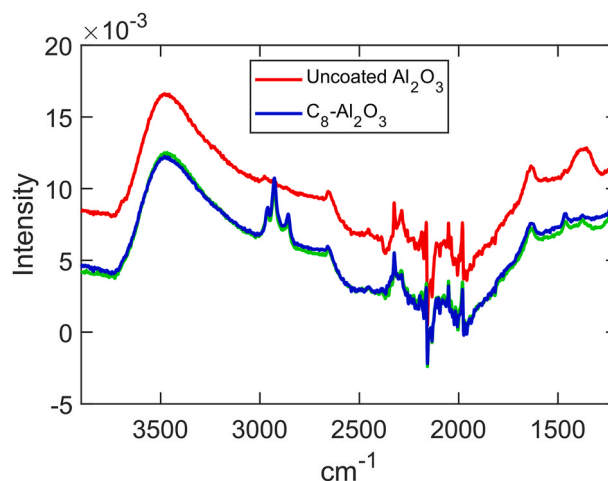**Fig. 2.** FTIR spectra (arbitrary units) of uncoated Al_2O_3 and C_8–Al_2O_3 nanoparticles. Double measurements were made for the C_8–Al_2O_3 nanoparticles (green and blue lines).

conductivity measurements were typically performed during 6 h.

The conductivity data were analysed with a filtering algorithm implemented in Matlab, which reduced the number of data-points by averaging the logarithmic conductivities within each desired time interval. For some of the nanocomposites, in particularly at 60 °C, the conductivity was close to the detection limit of the electrometer. At these low conductivities, the electrometer occasionally reported negative values of the signals instead of very small positive numbers. In the applied filtering protocol, these negative values were removed. As a consequence, the lowest measureable electrical conductivity was ca. $2 \cdot 10^{-17}$ S/m and the reported conductivities became upper bound values of the true values.

4. Results and discussion

Initially the nanoparticle powder was analysed to confirm a successful coating of the particles. Then the structure and the mechanical properties of the nanocomposites were examined to provide support towards the interpretation of the electrical data. Finally, the electrical conductivity of the nanocomposites was systematically assessed.
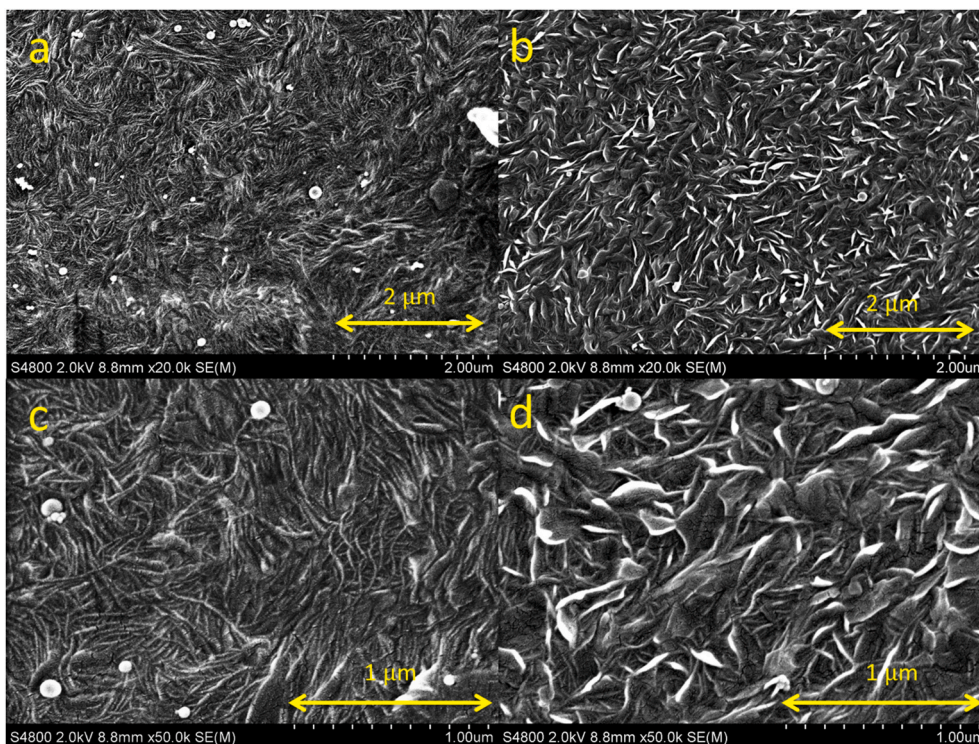
Fig. 3. SEM images of permanganate-etched 3 wt% C_8–Al_2O_3 nanocomposites with 0 wt% HDPE (left) and 4 wt% HDPE (right).
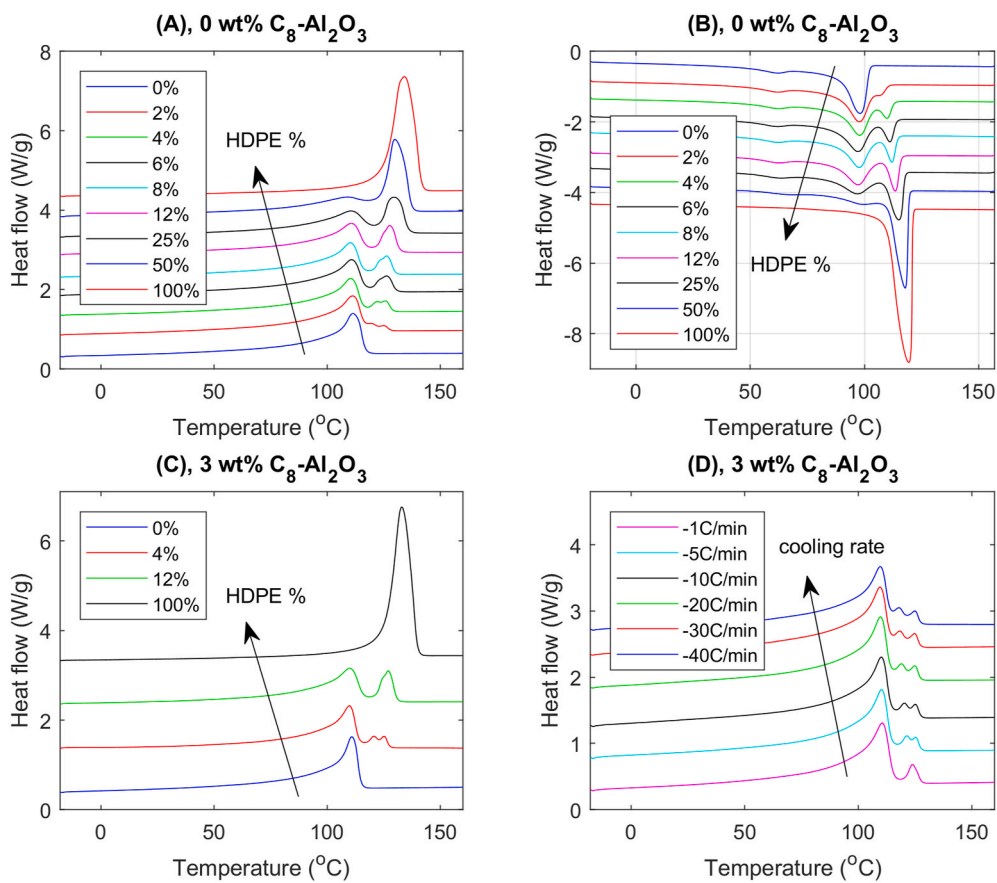

Fig. 4. DSC thermograms for LDPE with HDPE percentage from 0% to 100 wt%. **(A)** Second heating thermograms of LDPE/HDPE blends after cooling at 10 $^\circ$C/min from 160 $^\circ$C. **(B)** Cooling of the same blends before second heating. **(C)** Second heating thermograms of nanocomposites with 3 wt% C_8–Al_2O_3 after cooling with 10 $^\circ$C/min. **(D)** Second heating at different cooling rates (1–40 $^\circ$C/min) for a nanocomposite with 4 wt% HDPE and 3 wt% C_8–Al_2O_3.

4.1. Morphology of (octyl-coated) aluminium oxide nanoparticles

TEM micrographs (Fig. 1) showed that the Al_2O_3 nanoparticles in the silanized filler samples were surrounded by thin halos, indicating that the coating process had been successful. The visually observed thickness of the halo was 3–4 nm, which is somewhat larger than the length of a fully extended octyl chain (1.5 nm). The observed halo thickness is reasonable for a coating process with reactions involving silanes and surface hydroxyls and reactions between different silane molecules and is a consequence of using a triethoxy silane in an aqueous medium. The uncoated nanoparticles showed no halos. The average nanoparticle diameter was 50 ± 25 nm and the most common diameter was somewhat lower (40 nm) than the average diameter. A more detailed investigation of the size distribution and the dispersion of these nanoparticles in LDPE was previously presented [55].

IR revealed a distinct difference in IR-pattern between the coated and the uncoated nanoparticles (see Fig. 2). Only the octyl-coated particles had (C–H stretch) peaks around 2900 cm^{-1}, confirming the desired presence of an octyl layer coating [59]. Both IR and TEM thus showed that the aluminium oxide had been successfully coated with *n*-octyltriethoxysilane.

4.2. Characterization of LDPE/HDPE/C₈–Al₂O₃ nanocomposites

SEM revealed the nanoparticle dispersion and the crystal morphology in permanganate-etched nanocomposite fracture surfaces (Fig. 3). Overall, the nanoparticles in the 3 wt% C_8–Al_2O_3 nanocomposites were well dispersed, although small clusters containing 3–6 nanoparticles were present. The structure changed when 4 wt% HDPE was added, resulting in a more heterogeneous crystal morphology composed of dominant (HDPE) crystal lamellae blended with subsidiary (LDPE) crystal lamellae. The crystals were 5–30 nm in thickness, with thick HDPE crystals and thin LDPE crystals. Based on 200 measurements on each material, the average crystal width in the nanocomposite with 4 wt% HDPE was found to be significantly larger (240 ± 160 nm) than that in the corresponding material without HDPE (140 ± 100 nm). The addition of 3 wt% nanoparticles did not influence the crystal width significantly. The spherulite structures in LDPE are known to be effectively removed by extrusion [48], typically leading to a reduced electrical conductivity, eventually because the remaining spherulite boundaries become less effective conductive paths through the material.

DSC results for the cooling and the second heating of LDPE/HDPE blends and LDPE/HDPE/C₈–Al₂O₃ nanocomposites with 3 wt% nanoparticles are presented in Fig. 4. Two DSC measurements from −20 °C to 160 °C were performed on each sample. The LDPE gave rise to a single broad melting peak at ca. 110 °C and the HDPE had a single peak at ca. 130 °C (Fig. 4a). The curves for the LDPE/HDPE blends showed a gradual transition from that of LDPE to that of HDPE when the HDPE fraction increased, although the blends had two or three melting peaks rather than one. The highest and lowest peaks correspond to the melting of HDPE and LDPE respectively, whereas the middle peak arises from co-crystals and tends to disappear when cooling is too slow. The general trend agrees with previous studies [12], although we observed the three melting peaks for slightly lower HDPE fractions (2–4 wt%) than previously reported (5–10 wt%). The cooling curves before the second heating contained double peaks but not triple peaks (Fig. 4b) and the addition of 3 wt% C₈–Al₂O₃ nanoparticles did not change the second heating DSC curves to any great extent (Fig. 4c). For the nanocomposite with 4 wt% HDPE and 3 wt% C₈–Al₂O₃, the effect of cooling rate in the interval from 1 °C/min to 40 °C/min was examined (Fig. 4d). With a low cooling rate (1 °C/min), the material was given enough time to phase separate, thus eliminating the amount of the co-crystals and the corresponding peak from the thermogram [12]. The crystallinities of LDPE and HDPE were 49 and 81%, respectively, whereas the crystallinity of the blends increased linearly with increasing HDPE fraction between these values. The nanoparticles had only a small effect on the
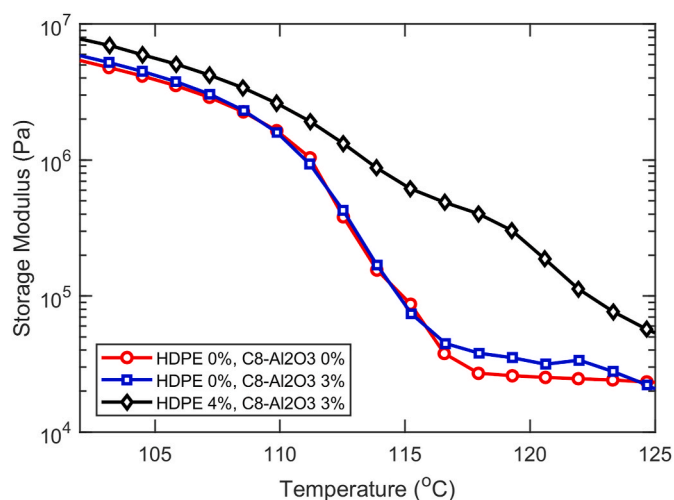

Fig. 5. Storage modulus (G′) versus temperature for nanocomposites and pure LDPE.

crystallinity, the maximum change in crystallinity with the addition of nanoparticles being only 3%. For the nanocomposite with 4 wt% HDPE and 3 wt% C₈–Al₂O₃, all cooling rates between 30 °C/min and 5 °C/min resulted in crystallinities between 50% and 52%. A faster cooling (40 °C/min) resulted in a lower crystallinity (45.7%) and a slower cooling (1 °C/min) resulted in a higher crystallinity (56.4%). The crystal thickness L_c was assessed through the Thomson-Gibbs equation, with material constants from Wunderlich 1980 [60,61].

$$L_c = 0.624 T_{m0}/(T_{m0} - T_m) \quad (4)$$

where T_m is the melting temperature (measured with DSC) and $T_{m0} = 414.2$ K is the reference melting point. The melting temperature of the LDPE was 111.3 °C, corresponding to a crystal thickness of 8.7 nm, and the melting temperature of HDPE was 134.3 °C, corresponding to a crystal thickness of 38.3 nm.

In our previous work on LDPE/HDPE blends we have observed that adding HDPE results in co-crystallisation and leads to an increased number of tie-chains and trapped entanglements [12,18]. Further analysis was done with DMTA [62]. For pure LDPE, DMTA showed a sudden drop in the value of the storage (G′) and loss (G″) modulus immediately after the melting temperature (Fig. 5). The existence of the C₈–Al₂O₃ nanoparticles did not have any effect on the thermomechanical behaviour. By adding 4 wt% HDPE a clear plateau exists in the values of G′ and G″ in the region between the melting temperatures of the pure components. This indicates that the co-crystals and the resulting tie-chains and trapped entanglements lead to an increase of the mechanical stability and integrity of an otherwise molten material. This behaviour is similar to previously reported results on the same and different systems with varying microstructures [12,18]. From these results we can see that the existence of the nanoparticles had almost no effect on the thermomechanical properties of the overall matrix. These enhanced mechanical properties can reduce the need for crosslinking in electrical insulation applications and thereby facilitate recycling.

4.3. Electrical conductivity of LDPE/HDPE/C₈–Al₂O₃ nanocomposites

Fig. 6 shows a gradual decrease with time of the electrical conductivity at 32 kV/mm for different material compositions at 60, 70 and 90 °C. At 60 °C, the addition of 4 wt% HDPE to the LDPE matrix resulted in a decrease in conductivity of nearly one order of magnitude after 6 h. The addition of 2 wt% HDPE resulted in a smaller but still distinct improvement. The addition of 3 wt% octyl coated Al₂O₃ to the LDPE gave a decrease in conductivity of more than two orders of magnitude, which is in accordance with previous measurements [13]. The
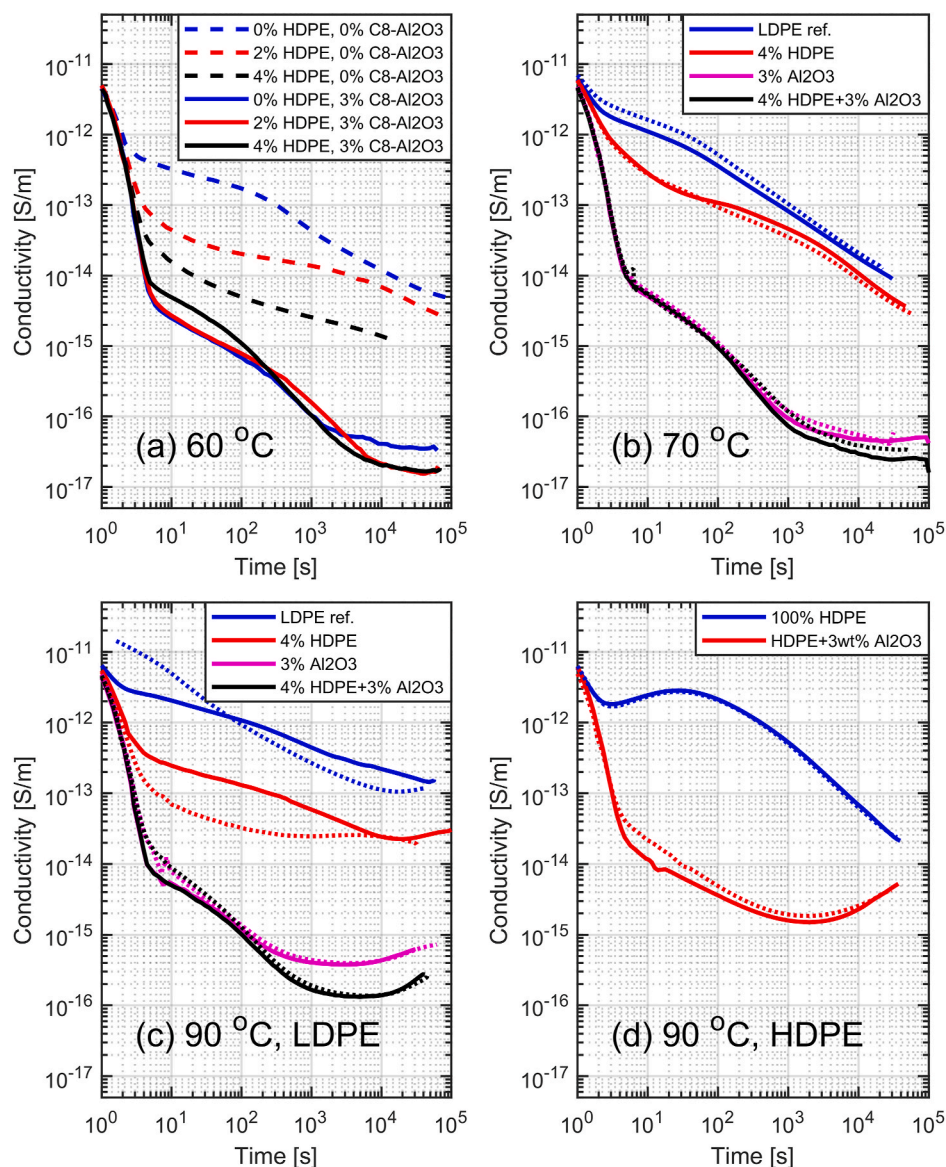
Fig. 6. Conductivity versus time for different materials. (a) 60 °C, (b) 70 °C, (c–d) 90 °C. The dotted curves in b-d are replicates of the same material compositions. Fig. 6a–c are for LDPE based nanocomposites whereas Fig. 6d show HDPE and HDPE +3 wt% C_8–Al_2O_3.

three-component material (3 wt% C_8–Al_2O_3 and 2 or 4 wt% HDPE) showed a further decrease by a factor 2, compared to the binary 3 wt% C_8–Al_2O_3 nanocomposite. Almost identical results were obtained with 1.5 wt % nanoparticles, confirming that the optimum at 3 wt% nanoparticles [13] is insensitive to small deviations in filler content. At 60 °C, the reduction in conductivity for the ternary composites would be more pronounced with a lower detection limit of the electrometer. The reported conductivities cannot go below the detection limit (ca. $2 \cdot 10^{-17}$ S/m) and thus represent upper bounds of the true conductivities. The conductivity curves at 70 and 90 °C followed the same general trends as that at 60 °C, but the absolute values increased with increasing temperature. Two measurements were made for each material composition, confirming that the difference between measurements was clearly smaller than the differences between the different materials. At 90 °C, a slight increase in conductivity was observed by the end of the measuring period for all the LDPE-based materials, probably due to temperature-induced aging of the samples. The addition of 4 wt% HDPE resulted in a conductivity drop by a factor of two (6h, 70 °C) or three (6h, 90 °C), both with and without nanoparticles. Previous studies [10] have reported a larger effect on the conductivity when adding HDPE to

LDPE at 70 °C, but our trend is clearly similar.

The time-dependent conductivity curves shown in Fig. 6 can be divided into 3 time-regions [63]: (1) the capacitive charging current region, (2) the absorption current region, comprising two sub-regions and (3) the quasi steady-state region.

A capacitive charging current will flow through the material once the voltage is applied, causing a distinct spike in the measured current. Before the voltage is applied, the current is always close to zero. Since the peak value is used as the starting point of each conductivity curve, the preceding capacitive current increase is not shown explicitly in the figures.

The absorption current region, which is characterized by a rapid decrease in apparent conductivity, starts immediately after the capacitive current peak. In a log-log diagram, the decrease is approximately linear and can be described with Curie-von Schweidler's law [63]: $\sigma(t) \propto I(t) = A t^{-b_n}$, with charging time t, current $I(t)$, temperature-dependent pre-factor A and slope b_n. The initial slope was highest for the nanocomposites ($b_n \approx 4$), but was notable also for the pure polymers ($1 < b_n < 4$). After a short period of time, ca. 5 s, a transition with a sharp shift in slope occur, typically from $b_n \approx 4$ to $b_n \approx 0.6$.
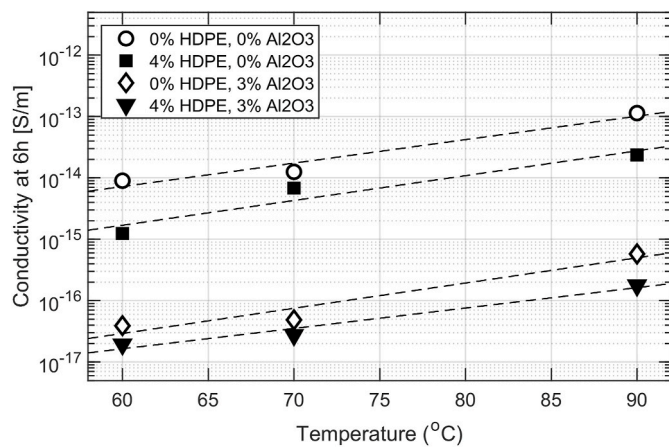
Fig. 7. Conductivity at 6 h versus temperature for 4 materials. The straight lines are best fits to the experimental conductivity data in lin-log scale. The lowermost conductivities at 60 and 70 °C are near the detection limit of the electrometer and should thus be even lower.

Fig. 8. Electrical conductivity (6h, 90 °C, 32 kV/mm) as a function of HDPE wt. %, for LDPE blends with and without 3 wt% C_8–Al_2O_3 in the LDPE.

The transition time, as well as the slope, depends on the polarization field [64]. After the transition, the absorption current region continues for approximately 1 h. Charge-accumulation, electrode polarization, dipole orientation, trapping of charge carriers (electrons, holes, ions and polar molecules) in deep traps and tunnelling/hopping of charge carriers between shallow traps are some of the electrical mechanisms influencing the absorption current region [65]. The reduction in conductivity when adding nanoparticles to LDPE can be associated with the trapping of charge carriers at nanoparticle surfaces [8,29,66] whereas the reduction in conductivity when adding HDPE to LDPE can be linked with the morphological changes and the resulting crystal structure [10].

A quasi-steady state arises once the absorption current has settled. For polymers at high electric fields, a completely steady state is however difficult to achieve within the practical experimental limitations, because the polymer itself changes with time, especially at elevated temperatures. Effects caused by thermal aging, including oxidation, polymer relaxation and redistribution of polar molecules, have a significant influence on the apparent conductivity of the materials [5]. Thus, when comparing conductivities, it is crucial to control both the electrical- and thermal history, indicating the importance of detailed and controlled sample preparation procedures. Thermal conditions influence all conductivity measurements, but are particularly important during prolonged experiments at elevated temperatures. Heating of polymers in air can cause oxidation. At low temperatures, a slight oxidation of LDPE decreases the conductivity, whereas a strong oxidation increases the conductivity [48]. At elevated temperatures, oxidation generally increases the conductivity, which is one probable cause for the slight increase observed at the end of the conductivity curves, especially at 90 °C (Fig. 6c–d). One important conclusion is that long-term conductivity measurements should preferably not be performed in air, in order to avoid oxidation and to mimic the conditions that HVCD cables operate.

The findings from Fig. 6 are summarized in Fig. 7, where the logarithmic electrical conductivity (6 h, 32 kV/mm) of four materials (LDPE, LDPE+4 wt% HDPE, LDPE+3 wt% C_8–Al_2O_3 and LDPE+4 wt% HDPE+3 wt% C_8–Al_2O_3) is shown to be linearly dependent on the temperature, the slopes of the lines being approximately the same for all four materials. The effect of adding HDPE to the pure LDPE was similar to the effect of adding HDPE to the two-component nanocomposites. The conductivity reduction resulting from the presence of nanoparticles and HDPE can therefore be considered additive. As a consequence, the three-component composite has an insulating capacity superior to that of two-component materials. This implies that two independent conductivity-reduction mechanisms are involved when HDPE and nanoparticles are
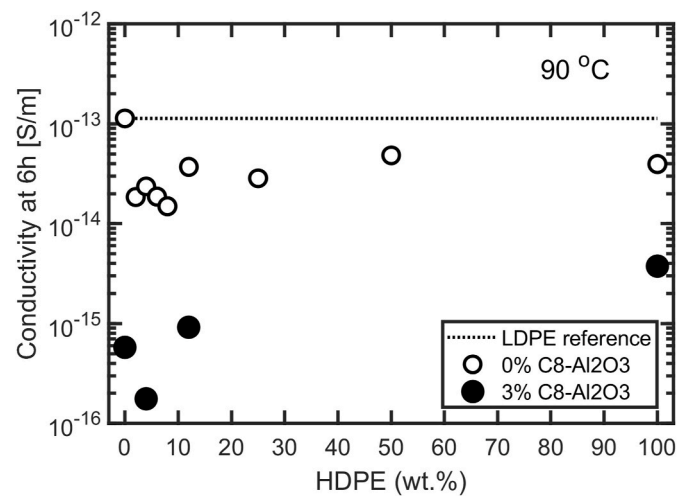
added to the LDPE and thus that the matrix material and the nanoparticles can be optimized independently before they are added together.

In order to investigate the optimal concentration of HDPE, the electrical conductivity (6 h, 90 °C) of the LDPE/HDPE blends was measured as function of HDPE content with and without 3 wt% nanoparticles (Fig. 8). The optimal concentration was observed between 4 and 8 wt % HDPE, both with and without nanoparticles. The conductivity of the pure HDPE was slightly higher than that of the optimal 4–8 wt% LDPE/HDPE blends. This can probably be associated to the lower cleanliness of the HDPE and the differences in the overall morphology of the two systems [6,8]. The decrease in conductivity was smaller when nanoparticles were added to HDPE than to LDPE, probably due to an influence of the crystal structure.

Commercial state-of-the-art HVDC cables contain chemically cross-linked polyethylene, whereas the system in our study is not. Cross-linking can be expected to have a minor effect on the overall electrical conductivity [10], but the improved thermomechanical properties after blending LDPE with small fractions of HDPE can in principle provide the necessary stability to reduce the overall crosslinking requirements. Furthermore, it is worth noticing that a wide range of crosslinking alternatives have been studied recently with very promising results [67–70].

5. Conclusions

In previous work, it was concluded that the electrical conductivity of LDPE can be significantly reduced by adding small fractions of either HDPE or metal-oxide nanoparticles such as octyl-coated aluminium oxide. The hypothesis was that the reductions in conductivity due to the two additives are the results of two different physical mechanisms and, as a consequence, that an additive effect would be observed when the two concepts were combined. LDPE/HDPE polymer blends with and without C_8–Al_2O_3 nanoparticles have therefore been manufactured and their conductivity has been measured at 60, 70 and 90 °C, using a voltage of 32 kV/mm. At all temperatures, the addition of 4 wt% HDPE to the LDPE resulted in a moderate decrease in conductivity (~2–10 times), while the addition of 3 wt% C_8–Al_2O_3 caused a larger drop (~200 times). At 90 °C, the optimal HDPE concentration was found to be between 4 and 8 wt%. When 4 wt% HDPE was added to the composite with 3 wt% nanoparticles, an additional decrease (~3 times) was observed, confirming that the composite material had a significantly lower electrical conductivity. Since the contributions to the reduction in conductivity from the HDPE and nanoparticles were additive, the two

contributions must stem from different physical mechanisms. Ternary composites can therefore be further optimized either by adjusting the polyethylene blend or the nanoparticles. Adding HDPE in LDPE has been reported to offer increased thermomechanical behaviour. In this work we have seen that adding nanoparticles does not alter this behaviour. This has the potential to lead to a system with some degree of physical crosslinking, thus reducing the need of chemical crosslinking with peroxides. Finally, the additivity of the reductions in conductivity when combining nanoparticles, HDPE and LDPE indicates the immense potential for further optimization of such systems in the future, because the particles and the polymer matrix can be improved nearly independently.

CRediT authorship contribution statement

Fritjof Nilsson: Conceptualization, Methodology, Software, Validation, Formal analysis, Investigation, Data curation. **Mattias Karlsson:** Resources, Methodology, Validation, Writing - review & editing. **Ulf W. Gedde:** Funding acquisition, Writing - review & editing. **Roland Kádár:** Resources, Investigation. **Karolina Gaska:** Investigation. **Christian Müller:** Resources, Writing - review & editing. **Per-Ola Hagstrand:** Resources, Writing - review & editing. **Richard T. Olsson:** Validation. **Mikael S. Hedenqvist:** Resources, Methodology, Writing - review & editing. **Thomas Gkourmpis:** Resources, Methodology, Writing - review & editing.

Declaration of competing interest

The authors declare that they have no known competing financial interests or personal relationships that could have appeared to influence the work reported in this paper.

Acknowledgements

References

[1] Chen G, Hao M, Xu Z, Vaughan A, Cao J, Wang H. Review of high voltage direct current cables. CSEE J Power and Energy Systems 2015;1(2):9–21.

[2] Hanley TL, Burford RP, Fleming RJ, Barber KW. A general review of polymeric insulation for use in HVDC cables. IEEE Electr Insul Mag 2003;19(1):13–24.

[3] Fothergill JC. "The coming of age of HVDC extruded power cables,". Electrical Insulation Conference (Eic) 2014:124–37.

[4] Ghorbani H, Gustafsson A, Saltzer M, Alapati S. "Extra high voltage DC extruded cable system qualification A world record in HVDC cable technology,". International Conference on Condition Assessment Techniques in Electrical Systems (CATCON) 2015:236–41.

[5] Ghorbani H, Christen T, Carlen M, Logakis E, Herrmann L, Hillborg H, Petersson L, Viertel J. "Long-term conductivity decrease of polyethylene and polypropylene insulation materials," IEEE trans. Dielectr. Electr. Insul., vol. 24, no 2017;3:1485–93.

[6] Pallon L, Hoang A, Pourrahimi A, Hedenqvist M, Nilsson F, Gubanski S, et al. The impact of MgO nanoparticle interface in ultra insulating polyethylene nanocomposites for high voltage DC cables. J Mater Chem 2016;4(22):8590–601.

[7] Pourrahimi AM, Hoang TA, Liu D, Pallon LK, Gubanski S, Olsson RT, et al. Highly efficient interfaces in nanocomposites based on polyethylene and ZnO nano/hierarchical particles: a novel approach toward ultralow electrical conductivity insulations. Adv Mater 2016;28:8651–7.

[8] Pourrahimi AM, Olsson RT, Hedenqvist MS. "The role of interfaces in polyethylene/metal-oxide nanocomposites for ultrahigh-voltage insulating materials," *advanced materials*, 2017;1703624.

[9] Hjertberg T, Englund V, Hagstrand P, Loyens W, Nilsson U, Smedberg A. Materials for HVDC cables" REE. Revue del´ electricit´ e et de l´ electronique, no 2014;4.

[10] Andersson M, Hynynen J, Andersson M, Englund V, Hagstrand PA, Gkourmpis T, Müller C. Highly insulating polyethylene blends for HVDC power cables. ACS Macro Lett 2017;6(2):78.

[11] Lin Y, Du W, Tu D, Zhong W, Du Q. Space charge distribution and crystalline structure in low density polyethylene (LDPE) blended with high density polyethylene (HDPE). Polym Int 2004;54:465–70.

[12] Andersson M, Hynynen J, Andersson M, Hagstrand PA, Gkourmpis T, Müller C. "Additive-like amounts of HDPE prevent creep of molten LDPE: Phase behaviour and thermo-mechanical properties of a melt miscible blend. J Polymer Sci B: Polymer Physics 2017;55:146–56.

[13] Liu D, Hoang A, Pourrahimi A, Pallon LK, Nilsson F, Gubanski S, Olsson RT, Hedenqvist M. Gedde UW*. Influence of nanoparticle surface coating on electrical conductivity of polyethylene/aluminium oxide nanocomposites for HVDC cable insulations. IEEE Trans Dielectr Electr Insul 2017;24(3).

[14] Zhou Y, Peng S, Hu J, He J. Polymeric insulation materials for HVDC cables: development, challenges and future prespective. IEEE Trans. Dielectr. Electr. Insul 2017;24(3).

[15] Nageshwar RB, Nandakumar VS, Anju RK, Ashwin PC, Kandibran R. HVDC cable, LDPE nano dielectric and its response to low frequencies. IEEE international conference on high voltage engineering and application (ICHVE). 2018.

[16] Gao Y, Huang X, Min D, Li S, Jiang P. Recyclable dielectric polymer nanocomposites with voltage stablizer interface: toward new generation of high voltage direct current cable insulation. ACS Sustainable Chem Eng 2019;7:513–25.

[17] Gao Y, Xu B, Wang X, Jia T. Charge transport in low density polyethylene based micro/nano-composite with improved thermal conductivity. J Physics D: Applied Physics 2019;52:285–302.

[18] Andersson MG, Ständler R, Hagstrand PO, Müller C. Influence of molecular weight on the creep resistance of almost molten polyethylene blends. Macromol Chem Phys 2018;219:1700072.

[19] Wang S, Zha J, Wu Y, Ren L, Dang Z, Wu J. "Preparation, microstructure and properties of polyethylene/alumina nanocomposites for HVDC insulation,". IEEE Transactions on Dielectrics and Electrical Insulation December 2015;22(6):3350–6. https://doi.org/10.1109/TDEI.2015.004903. 092902.

[20] Wang SJ, Zha JW, Wu YH, Ren L, Dang ZM, Ji Wu. Preparation, microstructure and properties of polyethylene/aluminium nanocomposites for HVDC insulation. IEEE Trans. Dielectr. Electr. Insul 2015;22(6).

[21] Zha JW, Yan HD, Li WK, Zhang DL, Dang ZM. Sandwiched structure effect on space charge chargecteristics of aluminium/polyethylene nanocompomposites. IEEE Trans. Dielectr. Electr. Insul 2017;24(3).

[22] Yao Zhou, Hu J, Dang B, He J. Effect of different nanoparticles on tuning electrical properties of polypropylene nanocomposites. IEEE Trans. Dielectr. Electr. Insul 2017;24(3).

[23] Ciuprina F, Zaharescu T, Plesa I. Effects of γ-radiation on dielectric properties of LDPE-Al2O3 nanocomposites. Radiat Phys Chem 2013;84:145–50.

[24] Elimat ZM, Zihlif AM, Schulte KI. Vega A de la, Gagosta G. Electrical Characterization of polyethylene oxide alumina composite. J Thermoplastic composite materials 2011;26(2):176–92.

[25] Park YJ, Kwon JH, Sin JY, Hwang JN, Seo CW, Kim JH. DC conductivity and breakdown characteristics of Al2O3/crosslinked polyethylene nanocomposites for high voltage direct current transmission cable insulation. Japanese J Appl Phys 2014;53(8S3):08NL05.

[26] Panaitescu D, Ciuprina F, Iorga M, Frone A, Radovici C, Ghiurea M, Sever S, Plesa I. Effects of SiO2 and Al2O3 nanofillers on polyethylene properties. J Appl Polym Sci 2011;122:1921–35.

[27] Jose JP, Thomas S. Aluminia-clay nanoscale hybrid filler assembling in cross-linked polyethylene based nanocomposites: mechanics and thermal properties. Phys chem chemphys 2014;16:14730.

[28] Zhang S, Cao XY, Ma YM, Ke YC, Zhang JK, Wang FS. The effects of particle size and content on the thermal conductivity and mechanical properties of Al2O3/high density polyethylene (HDPE) composites. Polymer letters 2011;5(7):581–90.

[29] Nilsson F, Karlsson M, Pallon L, Giacinti M, Olsson RT, Venturi D, Gedde UW, Hedeqvist MS. Influence of water update on the electrical DC-conductivity of insulating LDPE/MgO nanocomposites. Compos Sci Technol 2017;152:11–9.

[30] Saiz F, Quirke N. "The excess electron in polymer nanocomposites." Phys. Chem. Chem. Phys. 2018;20:27528.

[31] Hosier I, Praeger M, Holt A, Vaughan A, Swingler S. On the effect of functionaliser chain length and water content in polyethylene/nano-silica nanocomposites: Part I–dielectric properties and breakdown strength. Nanotechnology 2015:1–13.

[32] Hosier I, Praeger M, Vaughan A, Swingler S. The effects of water on the dielectric properties of aluminium based nanocompsites. IEEE trans. nanotechnology 1017; 16(4):1–10.

[33] Praeger M, Hosier I, Holt A, Vaughan A, Swingler S. On the effect of functionaliser chain length and water content in polyethylene/nano-silica nanocomposites: Part II–Charge transport. Nanotechnology 2015:1–14.

[34] Hui L, Schadler LS, Nelson J. The influence of moisture on the electrical properties of crosslinked polyethylene/silica nanocomposites. Dielectrics and Electrical Insulation, IEEE Trans. Nanotechnology 2013;20(2):641–53.

[35] Liu D, Pourrahimi A, Pallon L, Sánchez CC, Olsson R, Hedenqvist M, et al. Interactions between a phenolic antioxidant, moisture, peroxide and crosslinking by-products with metal oxide nanoparticles in branched polyethylene. Polym Degrad Stabil 2016;125:21–32.

[3][6] Hoang A, Serdyuk Y, Gubanski S. Charge transport in LDPE nanocomposite Part II-computational approach. Polymers 2016;8:2073–4360.

[37] Tian F, Lei Q, Wang X, Wang Y. Efffect of deep trapping states on space charge suppression in polyethylene/ZnO nanocomposite. Appl Phys Lett 2011;99:142903.

[38] Kubyshkina E, Unge M, Jonsson BLG. Communication: band bending at the interface in polyethylene-MgO nanocomposite dielectric. J Chem Phys 2017;146 (5). 051101.

[39] Tanaka T, Imai T. Advances in nanodielectric materials over the past 50 years. IEEE Electr Insul Mag 2013;12. 0883–7554.

[40] Reed C. Advances in polymer dielectrics over the past 50 years. IEEE Electr Insul Mag 2013;29(4):58–62.

[41] Teyssedre G, Laurent C. Advances in high-field insulating polymeric materials over the past 50 years. IEEE Electr Insul Mag 2013;29(5):26–36.

[42] Plesa I, Nothinger PV, Schlögl S, Sumereder C, Muhr M. Review: properties of polymer composites used in high voltage applications. Polymers 2016;8:173.

[43] Plesa I, Nothinger PV, Stancu C, Wiesbrock F, Schlögl S. Review: polyethylene nanocomposites for power cable insulations. Polymers 2019;11:24.

[44] Chen L, Huan TD, Ramprasad R. Electronic structure of polyethylene: role of chemical, morphological and interfacial complexity. Sci Rep 2017;7:6128.

[45] Nilsson F, Lan X, Gkourmpis T, Hedenqvist M, Gedde U. Modelling tie chains and trapped entanglements in polyethylene. Polymer 2012;53(16):3594–601.

[46] Moyassari A, Mostafavi H, Gkourmpis T, Hedenqvist MS, Gedde UW, Nilsson F. Simulation of semi-crystalline polyethylene: effect of short-chain branching on tie chains and trapped entanglements. Polymer 2015;72:177–84.

[47] Moyassari A, Unge M, Hedenqvist M, Gedde UW, Nilsson F. First-principle simulations of electronic structure in semicrystalline polyethylene. J Chem Phys 2017;146(20).

[48] Karlsson M, Xu X, Hillborg H, Ström V, Hedenqvist MS, Nilsson F, Olsson R. Lamellae-controlled electrical properties of polyethylene – morphology, oxidation and effects of antioxidant on the DC conductivity. RSC Adv 2020;10(8):4698–709.

[49] Li X, Du GQ, Kang J, Tu DM. "Influence of microstructure on space charges of polypropylene,". J Polymer Sci B-Polymer Physics 2002;40(4):365–74.

[50] Li X, Cao Y, Du QG, Yin Y, Tu DM. "Charge distribution and crystalline structure in polyethylene nucleated with sorbitol,". J Appl Polym Sci 2001;82(3):611–9.

[51] Kolesov SN. "The influence of morphology on the electric strength of polymer insulation," *ieee Transactions on electrical insulation*, vol. 15, no 1980;5:382–8.

[52] Zha JW, Yan HD, Li WK, Dang ZM. Morphology and crystalline-phase-dependent electrical insulating properties in tailored polypropylene for HVDC cables. Appl Phys Lett 2016;109:222902.

[53] Green CD, Vaughan AS, Stevens GC, Pye A, Sutton SJ, Geussens T, Fairhurst MJ. Thermoplastic cable insulation comprising a blend of isotactic polypropylene and a propylene-ethylene copolymer. IEEE Trans. Dielectr. Electr. Insul 2015;22(2): 639–48.

[54] Liu D, Pourrahimi AM, Pallon LKH, Andersson RL, Hedenqvist MS, Gedde UW, Olsson RT. Morphology and properties of silica-based coatings with different functionalities for Fe3, ZnO and Al2O3 nanoparticles. RSC Adv 2015;5:48094.

[55] Liu D, Pourrahimi AM, Olsson RT, Hedenqvist MS, Gedde UW. Influence of nanoparticle surface treatment on particle dispersion and interfacial adhesion in low-density polyethylene/aluminium oxide nanocomposites. Eur Polym J 2015;66: 67–77.

[56] Gray AP. "Polymer crystallinity determinations by DSC". Thermochim Acta 1970;1: 563–79.

[57] Wunderlich B, Bauer H. "Heat capacities of linear high polymers," adv. Polym. Sci. 1970;7:151.

[58] Wunderlich B. "Heat of fusion of polyethylene", J polymer sci. Part A2 1967;5.

[59] Coates J, Meyers RA. Interpretation of infrared spectra, a practical approach. In: Encyclopedia of analytical chemistry; 2006.

[60] Wunderlich B. Macromolecular physics. In: Crystal melting. vol. 3. New York and London: Academic press; 1980.

[61] Gedde UW, Hedenqvist MH. Fundamental polymer science, 2Ed. Springer nature. 2020.

[62] Menard KP. Dynamic mechanical analysis: an introduction. second ed. Boca Raton, FL: CRC Press; 2008.

[63] Lau KY, Vaughan AS, Chen G, Hosier IL, Ching KY, Quirke N. "Polyethylene/silica nanocomposites: absorption current and the interpretation of SCLC" Journal of physics. D. Appl Phys 2016;49(29):295–305.

[64] Mazur K. "Dielectric absorption, current-voltage characteristics and charge decay in PMMA/BaTiO/sub 3/ composites,". Proceedings of 1995 IEEE 5th International Conference on Conduction and Breakdown in Solid Dielectrics, Leicester, UK 1995: 98–102. https://doi.org/10.1109/ICSD.1995.522957.

[65] Das Gupta DK, Joyner K. "On the nature of absorption currents in polyethyleneterephthalate (PET)" Journal of Physics D: Applied Physics 9 1976; 829.

[66] Holder SL, Karlsson ME, Olsson RT, Hedenqvist MS. Nilsson F*. "Solubility and Diffusivity of Polar and Non-Polar Molecules in Polyethylene-Aluminum Oxide Nanocomposites for HVDC Applications." Energies 2020;13(3):722.

[67] Mauri M, Peterson A, Senol A, Elamin K, Gitsas A, Hjertberg T, Matic A, Gkourmpis T, Prietod O, Müller C. "Byproduct-free curing of a highly insulating polyethylene copolymer blend: an alternative to peroxide crosslinking". J Mater Chem C 2018;6:11292.

[68] Mauri M, Hofmann A, Gómez-Heincke D, Kumara S, Pourrahimi AM, Ouyang Y, Hagstrand PO, Gkourmpis T, Xu X, Prieto O, Müller C. Click chemistry-type crosslinking of a low-conductivity polyethylene copolymer ternary blend for power cable insulation. Polym Int April 2020;69(4).

[69] Ouyang Y, Mauri M, Pourrahimi AM, Östergren I, Lund A, Gkourmpis T, Prieto O, Xu X, Hagstrand PO, Müller C. "Recyclable polyethylene insulation via reactive compounding with a maleic anhydride-grafted polypropylene". ACS Appl. Polym. Mater 2020;2(6):2389–96.

[70] Kumara S, Xu X, Hammarström T, Ouyang Y, Pourrahimi AM, Müller C, Serdyuk YV. "Electrical characterization of a new crosslinked copolymer blend for DC cable insulation". Energies 2020;13(6):1434.